이학석사 학위논문

담도암에서 히스톤 탈아세틸화 효소6 저해로 인한 종양생장 억제 및 세포자멸사에 관한 분자생물학적 기전 연구

Glucose-regulated Protein 78 Acetylation by Histone Deacetylase 6 Inhibition Suppresses Proliferation and Promotes Apoptosis in Cholangiocarcinoma

울 산 대 학 교 대 학 원

의 학 과

김 초 롱

담도암에서 히스톤 탈아세틸화 효소6 저해로 인한 종양생장 억제 및 세포자멸사에 관한 분자생물학적 기전 연구

지 도 교 수 김 규 표

이 논문을 이학석사학위 논문으로 제출함

2020년 8월

울 산 대 학 교 대 학 원

의 학 과

김 초 롱

김초롱의 이학석사학위 논문을 인준함

심사위원 유 창 훈 (인)

심사위원 홍 승 모 (인)

심사위원 김 규 표 (인)

울 산 대 학 교 대 학 원

2020년 8월

Contents

List of Figures

Abstract

Histone deacetylase 6 (HDAC6) acts as a positive regulator to cellular protective responses of cancer cells in cancer progression. Eventually, HDAC6 is overexpressed in tissues from patients with various cancer. So, HDAC6 is an emerging therapeutic target for cancer.

We identified the molecular mechanisms of HDAC6 which mediates deacetylation of Glucose-regulated protein 78 (GRP78) in cholangiocarcinoma (CCA) biology and validated the value of HDAC6 as a target for treatment of CCA.

CCA cell lines showed high sensitivity to ACY-1215, an HDAC6 inhibitor, than that of normal bile duct cell. And HDAC6 inhibition by ACY-1215 showed increased cell mortality and apoptosis approximately 50% compared to control due to the reduction of GRP78 located on the plasma membrane. ACY-1215 increased the acetyl-form of GRP78 by approximately 50% compared to control, which impaired the translocation of GRP78 to the plasma membrane. These modifications of GRP78 altered cellular proliferative signaling via PI3K/AKT. Furthermore, ACY-1215 suppressed tumor growth by 50% compared to vehicle control in a CCA animal xenograft model.

Our studies demonstrated that GRP78 acetylation by the inhibition of HDAC6 suppresses GRP78 translocation to the cell surface, which inhibits proliferation and

promotes apoptosis in CCA.

Keywords : Histone Deacetylase 6 (HDAC6), Cholangiocarcinoma (CCA), Glucose-regulated Protein 78 (GRP78), Acetylation, ACY-1215

Introduction

Cholangiocarcinoma (CCA) is a malignancy arising from the epithelial cells lining the bile ductal tree. Although surgical resection is the preferred curative treatment of CCA, it is restricted to patients with early stage-CCA. Based on the ABC-02 phase III clinical study, gemcitabine and cisplatin are used as the standard care for patients with advanced biliary tract cancer (BTC). However, significant positive therapeutic outcomes have not been achieved [1].

In recent years, histone deacetylase (HDAC), which catalyzes the deacetylation of proteins, has become an emerging therapeutic target for CCA. HDAC contributes to the proliferation, invasion, metastasis, migration and chemoresistance of CCA through epigenetic regulation. These effects are suppressed by pan-HDAC inhibitors, including vorinostat, trichostatin A, and CG200745 [2-4]. Among the various types of HDAC, HDAC6 has been highlighted as a cancer therapy target. This is because HDAC6 is specifically localized in the cytosol, and its substrates, include α-tubulin, heat shock protein 90, and glucose-regulated protein 78 (GRP78). Gradilone et al. have reported HDAC6 is overexpressed in tissues from patients with CCA, and it induces tumorigenesis by regulating ciliary function in CCA [5].

Due to the rapid growth of cancer cells and limited vascularization, the tumor environment undergoes stress conditions (e.g. hypoxia, nutrient deprivation and acidosis), which leads to prolonged ER stress in cancer cells. To alleviate ER stress and maintain ER homeostasis, the ER chaperones are involved in the degradation of unfolded or misfolded proteins, attenuation of protein synthesis, and induction of Unfolded Protein Response (UPR) genes.

One of the most characterized ER chaperones is GRP78. Although it was first identified in the ER lumen, recent studies have demonstrated that GRP78 is ubiquitous throughout the cell in the mitochondria, nuclei, plasma membrane, cytoplasm, and extracellular environment. The roles of GRP78 are different according to subcellular locations [6-8]. A cytoplasmic isoform of GRP78 (GRP78va) is overexpressed in leukemia cells and contributes to their survival [9]. GRP78 in the nuclei play a role in blocking DNA-damage-induced apoptosis in hepatoma cells [6, 10]. Furthermore, the GRP78 secreted by colon cancer and HCC cells promotes cell proliferation [11, 12].

Interestingly, several studies have shown that GRP78 is translocated to the plasma membrane in various cancer types. Cell surface GRP78 (cs-GRP78) has important roles in cell proliferation, metastasis, migration, invasion, apoptosis resistance and chemoresistance in many types of cancer cells [13, 14]. The cs-GRP78 is an α2-macroglobulin signaling

receptor, transmitting signals that increase the motility of prostate cancer cells [15]. Moreover, a specific anti-GRP78 antibody suppressed the function of cs-GRP78 and inhibited breast cancer cell proliferation and migration [16].

So far, the role of HDAC6 and GRP78 in tumor biology has been described in various cancers; however, the relationship between HDAC6 and GRP78 is still unclear in CCA. In this study, we identified the role of HDAC6 and GRP78 in CCA and validated HDAC6 inhibition as a target for treatment of CCA.

Materials and Methods

Cell lines and culture

The human CCA cell lines SNU-245, SNU-308 and SNU-1196 were purchased from the Korean Cell Line Bank (Seoul, Korea). The human CCA cell lines SSP-25 and TFK-1 were obtained from Center for Advancing Cancer Therapeutics (Seoul, Korea). The cells were cultured in RPMI-1640 medium (Gibco, USA) supplemented with 10% fetal bovine serum (WELGENE, Korea) and 1% penicillin/streptomycin (Gibco). The human cholangiocyte cell line MMNK-1 was obtained from the JCRB Cell Bank, National Institute of Biomedical Innovation, Health, and Nutrition (Japan). The cells were cultured in DMEM containing 5% fetal bovine serum and 1% penicillin/streptomycin. All of the cells were maintained in an incubator at 37℃, 5% CO_2.

Co-Immunoprecipitation

Cells were lysed in Cell Extraction Buffer (Invitrogen, USA) containing a protease inhibitor cocktail (Roche, Swiss). Then, 1 mg protein from the whole-cell lysates was precleared with 30 μl of Pierce Protein A/G agarose (Thermo Scientific, USA) in a rotator for 3 h at 4℃, followed by centrifugation at 2,500 rpm for 5 min at 4℃. The supernatant was mixed with 2 μg of GRP78 (ab21685; Abcam) or acetylated-Lysine (#9441; Cell

Signaling) and incubated in a rotator at 4°C overnight. Then, 50 μl of Pierce Protein A/G agarose was added, and it was further incubated in a rotator for 6 h at 4℃. The beads were pulled down by centrifugation and washed with Cell Extraction Buffer 5 times. The complex-bound beads were mixed with 100 μl of 4× LDS Sample Buffer (Invitrogen), followed by boiling for 5 min at 95℃ and centrifugation at 2,500 rpm for 5 min.

Cell surface protein biotinylation assay

After removal of the used medium, the cells were washed with ice-cold PBS twice. EZ-link Sulfo-NHS-LC-Biotin (Thermo Scientific) in ice-cold PBS at 0.25 mg/ml was applied to couple the surface protein with biotin (10 ml/100 mm plate), and the plate was gently shaken for 30 min at 4℃. To stop the biotinylation reaction, quenching solution (Thermo Scientific) was added, and the plate was tipped back and forth. The cells were scraped into the solution and transferred to a conical tube. Then, the cells were rinsed with ice-cold TBS twice and lysed in lysis buffer (Thermo Scientific) containing a protease inhibitor cocktail (Roche). During incubation, the cells were sonicated using five 1-second bursts at 1.5-low power to enhance the solubilization efficiency. The lysates were treated with NeutrAvidin Agarose (Thermo Scientific) for 1 h at room temperature to purify the surface proteins. The beads were then washed with washing buffer (Thermo Scientific)

containing a protease inhibitor cocktail and centrifuged at 1000 × g for 1 min 4 times. The contents were added with 400 μl of 4× LDS Sample Buffer (Invitrogen), followed by heating for 5 min at 95℃. The surface proteins were collected by centrifuging at 1000 × g for 2 min.

Flow cytometry analysis

The expression levels of cell surface GRP78 were detected by flow cytometry. TFK-1 cells were harvested at a density of 1×10^6 cells/ml in cell staining buffer plus 0.5% BSA (Gibco) in PBS (Thermo Scientific). To reduce non-specific immunofluorescence staining, the cells were mixed with 1 μg of purified human Fc receptor binding inhibitor solution (Invitrogen), followed by incubation with an anti-GRP78 antibody (ab188878; Abcam) or rabbit IgG polyclonal (ab171870; Abcam) for 1 h at 4℃. The cells were gently mixed every 10 min during this procedure. After centrifugation at 400 × g for 5 min at 4℃, the cells were washed with cell staining buffer twice and incubated with goat anti-rabbit IgG (A21070; Life Technologies, USA) for 30 min at 4℃ in the dark. The cells were gently mixed every 10 min during this procedure, followed by resuspension in 200~300 μl of cell staining buffer. The cells were then analyzed using a FACS Canto II flow cytometer (BD Biosciences, USA) and FlowJo V10 software (FlowJo, USA). The FACS Canto II was

operated by the Flow Cytometry Core Facility, Research Development Support Center, Asan Medical Center.

Apoptosis assay

Annexin V/Propidium Iodide (PI) double staining was performed for apoptosis analysis. After treatment with ACY-1215, 1×10^6 cells were rinsed with PBS, followed by centrifugation at 300 × g for 10 min at 4℃. The cells were washed with 1 ml of 1× binding buffer (Miltenyi Biotec, Germany) twice and resuspended in 100 μl of 1× binding buffer, followed by staining with 10 μl of Annexin V-FITC (Miltenyi Biotec) for 30 min at room temperature in the dark. Then, 1 ml of 1× binding buffer was added to the cells, followed by centrifugation at 300 × g for 10 min at 4℃. Subsequently, the cells were resuspended in 500 μl of 1× binding buffer and mixed with 5 μl of propidium iodide (Miltenyi Biotec). The cells were incubated for a further 15 min at room temperature in the dark. The cells were then analyzed using a FACS Canto II flow cytometer (BD Biosciences) and FlowJo V10 software (FlowJo). The FACS Canto II was operated by the Flow Cytometry Core Facility, Research Development Support Center, Asan Medical Center.

Western blotting

Whole-cell lysates were prepared by heating in 4× LDS Sample Buffer (Invitrogen). The proteins were loaded into the wells of NuPAGE™ 4–12% Bis-Tris Protein Gels (Invitrogen) and separated using SDS-PAGE in MES SDS Running Buffer (Invitrogen). The proteins separated according to their molecular weight were transferred onto polyvinylidene difluoride membranes (Invitrogen) in transfer buffer (Novex, USA). The membranes were blocked by 5% skim milk or BSA in Tris-buffered saline containing Tween-20 (TBST) (iNtRON Biotechnology) on an orbital shaker for 1 h at room temperature. After incubation with primary antibodies overnight at 4℃, the membranes were rinsed with TBST 10 min each three times and then incubated with horseradish peroxidase conjugated secondary antibodies (Cell Signaling) for 1 h at room temperature on an orbital shaker. The membranes were rinsed with TBST for 10 min each three times, followed by treatment with Super Signal West Femto Stable Peroxide Buffer (Thermo Scientific) to enhance the signals and then detected by using a Chemiluminescence Imaging System (ATTO, Japan). The sources of the antibodies are listed below. Antibodies against α-tubulin (#2144), acetylated-lysine (#9441), acetyl-α-tubulin Lys40 (#5335), Akt (#4691), Bad (#9268), cleaved PARP (#5625), HDAC6 (#7558), phospho-Akt Ser473 (#4060), phospho-Akt Thr308 (#9275), phospho-bad Ser112 (#9291), phospho-bad Ser136 (#4366), and ubiquitin (#3936) were from Cell Signaling. β-actin (A5441) was from Sigma-Aldrich.

PERK (sc-377400) was from Santa Cruz (USA). Annexin-2/ANXA2 (ab41803), GRP78 (ab21685), and p-PERK Thr982 (ab192591) were from Abcam (UK). The numerical intensity of the bands was calculated using the program ImageJ v1.52a (National Institutes of Health, http://imagej.nih.gov/ij/).

Cell viability assay and IC_{50} assay

The cells were seeded in triplicate at a density of 2×10^3 cells in 50 μl per well of a 96-well plate and incubated for 24 h at 37℃. The ACY-1215 (Selleckchem, USA), gemcitabine, cisplatin, and oxaliplatin (Sigma-Aldrich, USA) were diluted with growth medium to 2× of their final concentration, followed by adding 50 μl of each drug solution to the cells. Then, 20 μl of CellTiter-Glo® Luminescent Cell Viability Assay solution (Promega) in 100 μl of culture medium was added into each well of the 96-well plate containing the cells. The contents were mixed for 2 min on an orbital shaker for cell lysis, followed by incubation at room temperature for 10 min to stabilize the luminescent signal. The solution (100 μl/well) was transferred to white 96-well plates, and then we read the luminescence with a PerkinElmer VICTOR X2. For cell growth analysis, the number of cells was normalized to the negative control (vehicle). For the half-maximal inhibitory concentration (IC_{50}), the cell viability data was plotted as the percentage inhibition against

the log value of the concentrations of the drug. The IC_{50} was determined using GraphPad Prism v5.01 (GraphPad Software).

Xenografts

The TFK-1 cells (5×10^6) were subcutaneously injected into the right flanks of 5-week-old BALB/c male nude mice (Central Laboratory Animal Inc., Korea). When the tumors reached approximately 80 to 150 mm3, the animals were randomized into vehicle control and ACY-1215 treatment groups of 7 mice each. The ACY-1215 (50 mpk) was diluted in 5% DMSO (Sigma-Aldrich)/45% PEG-400 (Daejung)/50% ddH_2O buffer and administered intraperitoneally 3~4 days/week for 3 weeks. The tumor size was measured twice a week and calculated by the formula (length × width × width)/2. After completing the last treatment, the mice were euthanized, and the tumors were harvested for analysis. All experiments were approved by the Institutional Animal Care and Use Committee of the Asan Institute for Life Science.

Immunohistochemistry

The tumor tissues embedded in paraffin were deparaffinized using EZ Prep (Roche), and then were rinsed with reaction buffer [Tris buffer (pH 7.6)] and treated with Cell Conditioner containing Tris/Borate/EDTA buffer (pH 8.4) for 60 min at 100℃. Then, the sections were incubated with 3% Ultraview peroxidase inhibitor (Roche) for 4 min at 37℃ to block the innate hydroperoxidases. The sections were incubated with anti-acetyl-α-tubulin Lys40 antibody (#5335; Cell signaling) and anti-Ki-67 antibody (#9027; Cell signaling) for 36 min at 37℃. After washing with reaction buffer, the sections were further incubated for 1 h with DISCOVERY UltraMap anti-Rb HRP antibody (Roche) for 16 min at 37℃, and then stained using an Ultra View Universal DAB Detection Kit (Roche). Finally, the sections were washed with reaction buffer and stained with hematoxylin (Roche). The images on the slides were visualized with an Olympus BX40 light microscope (Olympus, Japan) at ×40 magnification. The Immunohistochemistry was operated by the Center for Non-clinical Development, Research Development Support Center, Asan Medical Center.

Statistical Analysis

Statistical analysis was performed using two-sided standard Student's t-tests with GraphPad Prism v5.01 (GraphPad Software). A $P < 0.05$ was considered to be statistically significant. Data are presented as mean ± SEM.

Results

The CCA cell lines showed high sensitivity to the HDAC6 inhibitor

To check their sensitivity to ACY-1215, the only available oral HDAC6 inhibitor, its half-maximal inhibitory concentration (IC_{50}) values were defined in a normal bile ductal cell line, MMMK-1, and various CCA cell lines including SNU-245, SNU-308, SNU-1196, SSP-25, and TFK-1. All CCA cell lines were more sensitive to ACY-1215 than MMNK-1 (Fig. 1A). Then, to confirm the inhibitory effect of ACY-1215 on HDAC6 activity, the level of acetylation on α-tubulin was evaluated via western blot. The TFK-1 cells were cultured with ACY-1215 at 5, 10 and 20 μM for 24 hours. High levels of acetylated α-tubulin were detected in the ACY-1215 treatment group, indicating ACY-1215 effectively inhibited HDAC6 activity. However, ACY-1215 did not affect HDAC6 expression (Fig. 1B). In particular, among the CCA cell lines, the IC50 value of TFK-1 (IC_{50} = 11.62 μM) was approximately 6-fold lower than that of MMNK-1 (IC_{50} = 71.47 μM). These results indicated that the CCA cell lines had higher sensitivity to ACY-1215 than did the normal bile ductal cell line.

Figure 1

(A)

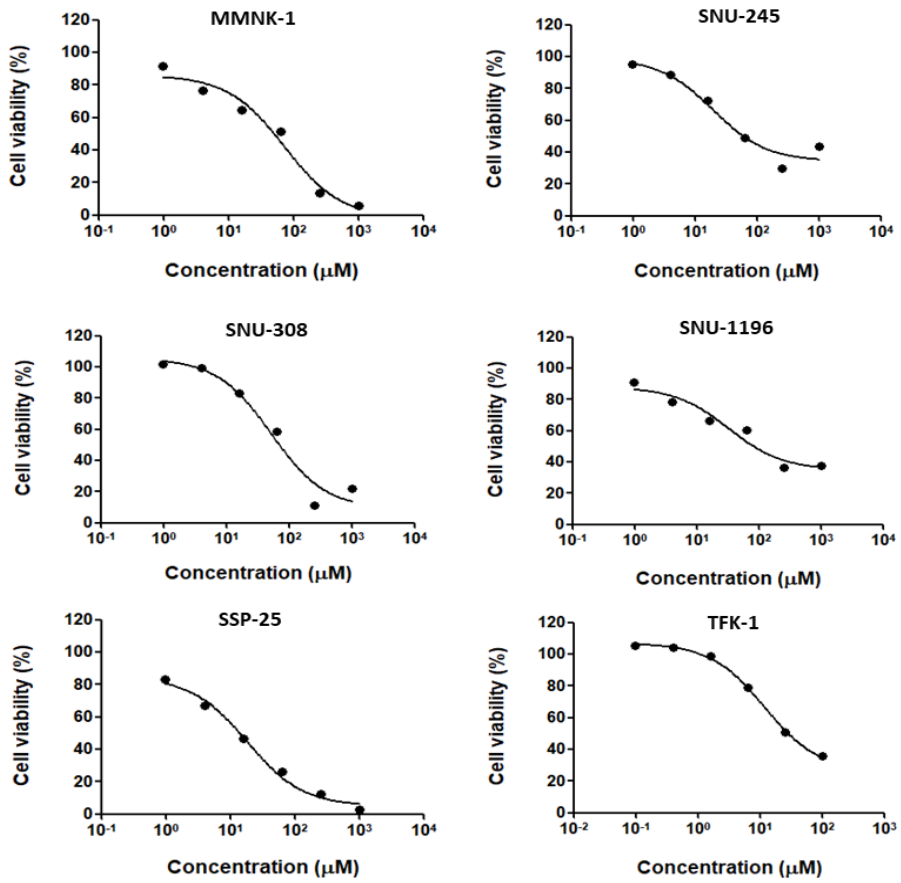

	MMNK-1	SNU-245	SNU-308	SNU-1196	SSP-25	TFK-1
IC_{50} (μM)	71.47	19.35	51.15	32.51	17.96	11.62

(B)

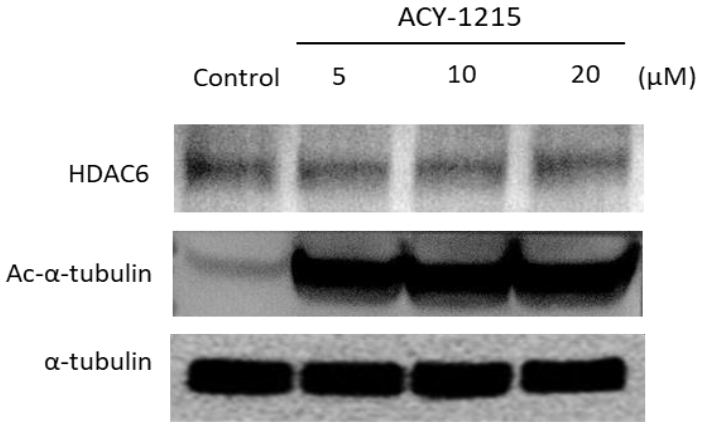

Figure 1. The CCA cell lines had high sensitivity to HDAC6 inhibitor. (A) IC_{50} curve and table of ACY-1215, HDAC6 inhibitor, in normal bile ductal cell line (MMNK-1), two extrahepatic CCA (SNU-245, TFK-1), gallbladder adenocarcinoma (SNU-308) and two extrahepatic CCA (SNU-1196, SSP-25). Cell viability was analyzed by CellTiter-Glo assay (n=3). (B) TFK-1 cells were treated with ACY-1215 at the indicated concentrations (5, 10 and 20 μM) for 24 hours. HDAC6, acetyl-α-tubulin and α-tubulin were detected by western blot.

HDAC6 inhibition resulted in cell death in CCA cell line

To evaluate whether HDAC6-targeted therapy using ACY-1215 is more effective than the established cytotoxic chemotherapy for CCA cell lines, the TFK-1 cells were treated for 24 hours with gemcitabine, cisplatin, or oxaliplatin at 100 μM, or ACY-1215 at 10 μM. The cisplatin and oxaliplatin showed 20~30% cell death efficacy. Unlike cisplatin and oxaliplatin, gemcitabine did not induce cell death. However, ACY-1215 had greater efficacy, with viability of only 50% (Fig. 2A). Furthermore, the effect of ACY-1215 on cell viability occurred in a dose-dependent manner (Fig. 2B). Besides, morphological changes were also induced by ACY-1215 (Fig. 2C). Taken together, these findings showed HDAC6 inhibition by ACY-1215 may induce death of TFK-1 cells.

Figure 2

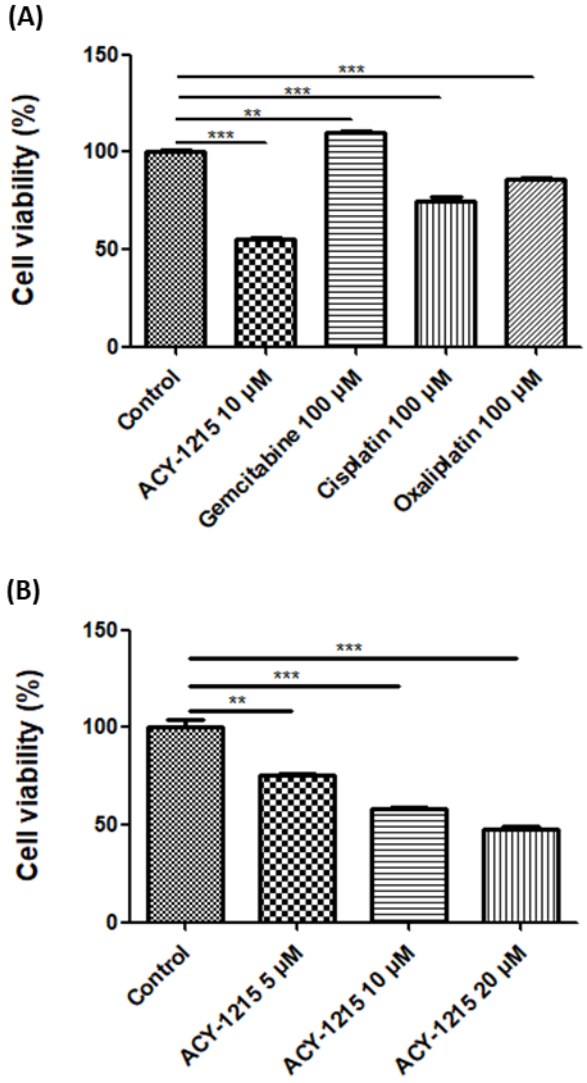
(A)
Cell viability (%)
150
100
50
0
***
***
**
***
Control
ACY-1215 10 μM
Gemcitabine 100 μM
Cisplatin 100 μM
Oxaliplatin 100 μM
(B)
Cell viability (%)
150
100
50
0
***
***
**
Control
ACY-1215 5 μM
ACY-1215 10 μM
ACY-1215 20 μM

(C)

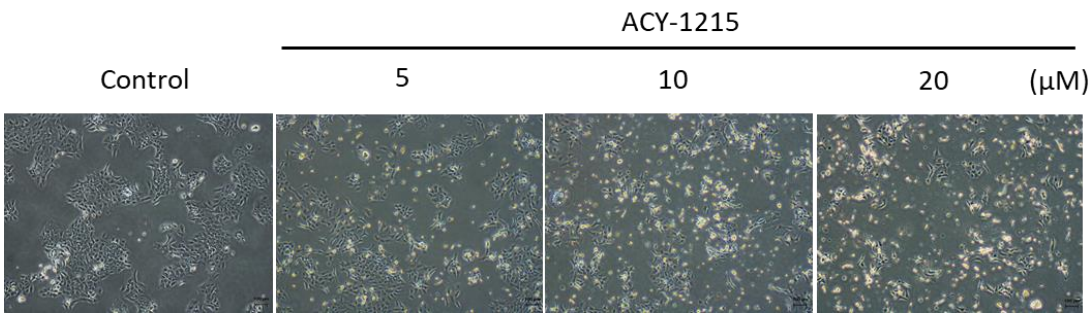
ACY-1215
Control
5
10
20
(μM)

Figure 2. HDAC6 inhibition resulted in cell death in CCA cell line. (A) One of CCA cell lines, TFK-1, was treated with several cytotoxic drugs (Gemcitabine, Cisplatin and Oxaliplatin) and ACY-1215, HDAC6 inhibitor, for 24 hours. Following that, cell viability was analyzed by CellTiter-Glo assay (n=3, $^{**}P < 0.01$, $^{***}P < 0.001$). (B) Dose-dependent decrease in cell viability by ACY-1215 at the indicated concentrations (5, 10 and 20 μM) for 24 hours. (C) Morphology of TFK-1 either untreated (Control) or treated with ACY-1215 (5, 10 and 20 μM) for 24 hours. All images were visualized at 4× magnification. Data are expressed as the Ave ± STDEV from three independent experiments (Scale bar = 100 μm, $^{*}P < 0.05$, $^{**}P < 0.01$ and $^{***}P < 0.001$ by two-tailed student's t-test).

HDAC6 inhibition induced apoptosis of CCA cell lines in a dose-dependent manner

To determine whether the death of TFK-1 cells induced by ACY-1215 is related to apoptosis, TFK-1 cells were cultured with various concentrations of ACY-1215 (5, 10 and 20 μM) for 24 hours followed by Annexin V/PI staining and flow cytometry analysis. The numbers of both early (Q4) and late (Q2) apoptotic cells were increased after treatment with ACY-1215 at 20 μM (25.6%) compared with the untreated cells (6.9%). The numbers of early apoptotic cells were significantly increased in a dose-dependent manner (Fig. 3A and 3B). Western blotting data showed up-regulated cleaved PARP protein following ACY-1215 treatment (Fig. 3C). These findings suggested that ACY-1215 induces apoptotic cell death in CCA cell lines.

Figure 3

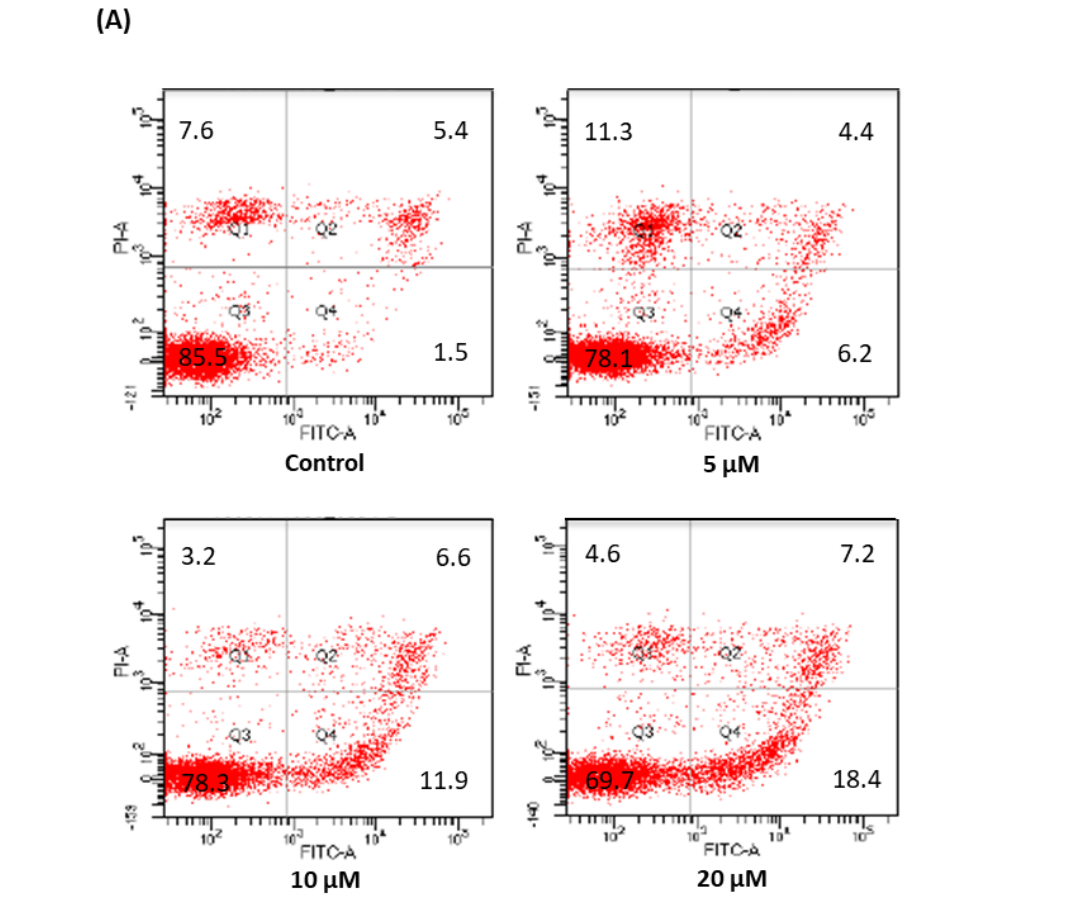
(A)
7.6
5.4
85.5
1.5
Control
11.3
4.4
78.1
6.2
5 μM
3.2
6.6
78.3
11.9
10 μM
4.6
7.2
69.7
18.4
20 μM
PI-A
FITC-A
Q1
Q2
Q3
Q4

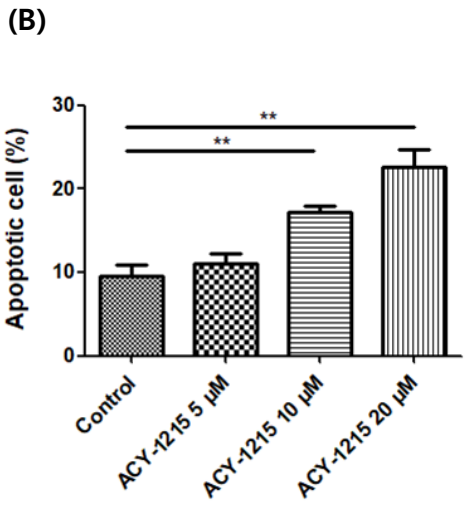
(B)
Apoptotic cell (%)
30
20
10
0
**
**
Control
ACY-1215 5 μM
ACY-1215 10 μM
ACY-1215 20 μM

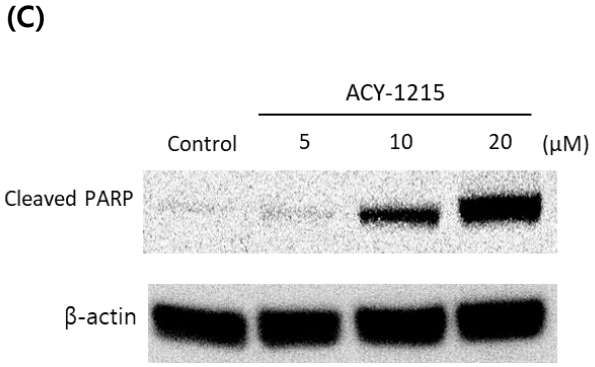
(C)
ACY-1215
Control
5
10
20
(μM)
Cleaved PARP
β-actin

Figure 3. HDAC6 inhibition resulted in apoptotic cell death. (A) Flow cytometry of apoptosis in TFK-1 cells treated with ACY-1215 at the indicated concentrations (5, 10 and 20 μM) for 24 hours. Apoptotic cells were increased in dose-dependent manner. (B) Dose course of apoptosis (n=3, $*P < 0.05$, $**P < 0.01$ versus the untreated group). (C) Cleaved PARP which represents apoptosis increased in dose-dependent manner of ACY-1215 in TFK-1 cells.

The novel role of GRP78 in the apoptosis signaling cascade under HDAC6 inhibition

Our observations showed that HDAC6 inhibition led to apoptosis of CCA cell lines. We next sought to determine how HDAC6 inhibition by ACY-1215 induces the apoptosis of cells. A previous investigation reported that HDAC6 is associated with ER stress [17, 18]. To determine whether the apoptosis induced by ACY-1215 was related to ER stress in CCA, we checked for changes in ER stress key regulators, including GRP78 and PERK, in TFK-1 cells. First, we checked the level of acetylation on α-tubulin as a pharmacodynamic marker for the activity of ACY-1215. The level of acetyl-α-tubulin was increased under ACY-1215 treatment, indicating the effective inhibition of HDAC6 activity by ACY-1215. Next, GRP78 was evaluated. The GRP78 expression was up-regulated two-fold at the highest dose of ACY-1215 (Fig. 4A). The level of phospho-PERK (its active form), another ER-stress regulator, was also increased under ACY-1215 treatment (Fig. 4B). However, the accumulation of ubiquitinated proteins, a surrogate feature of ER-stress, was not observed following ACY-1215 treatment (Fig. 4C). These data suggested that GRP78 has a distinct role in the apoptosis signaling cascade that is independent of ER stress under the HDAC6 inhibition condition induced by ACY-1215.

Figure 4

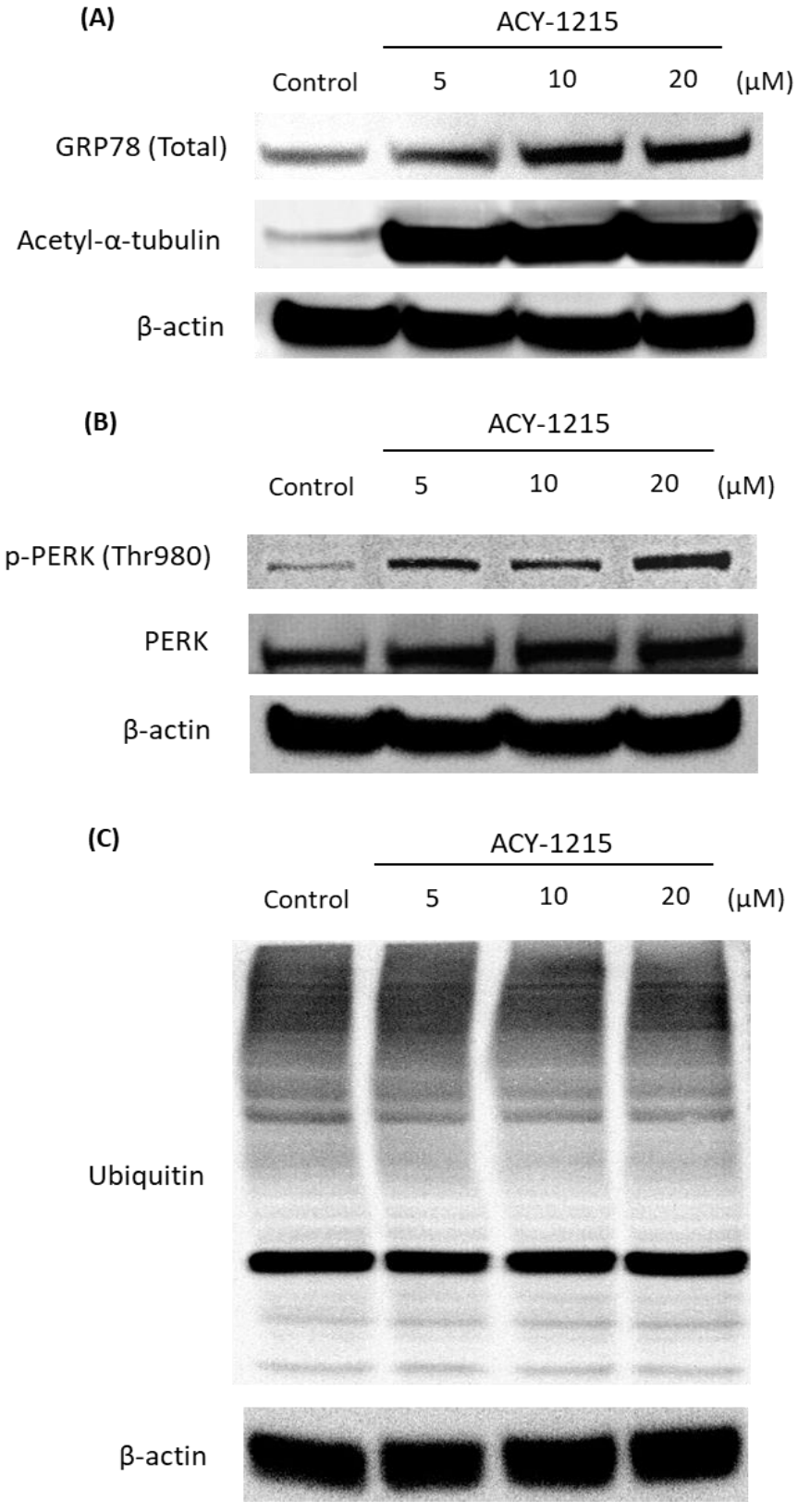
(A)
ACY-1215
Control
5
10
20
(μM)
GRP78 (Total)
Acetyl-α-tubulin
β-actin
(B)
ACY-1215
Control
5
10
20
(μM)
p-PERK (Thr980)
PERK
β-actin
(C)
ACY-1215
Control
5
10
20
(μM)
Ubiquitin
β-actin

Figure 4. HDAC6 inhibition increased ER stress but not ubiquitinated proteins. (A) Translational induction of GRP78 after treatment of ACY-1215 at the indicated concentrations (5, 10 and 20 μM) for 24 hours. Acetyl-α-tubulin indicates drug effect by ACY-1215. Data shown here represent one of three independent experiments. (B) Immunoblots of p-PERK (Thr980), PERK in TFK-1 lysates from cell treated with ACY-1215 (5, 10 and 20 μM). p-PERK (Thr980) serves as a marker for ER stress activation. (C) Ubiquitined proteins did not increase although ER stress was induced by ACY-1215. Data shown here represent one of three independent experiments.

HDAC6 inhibition suppressed translocation of GRP78 to the cell surface via the accumulation of acetylation on GRP78

After we checked the active status of ER-stress regulators under ACY-1215, we realized that GRP78 has a novel role in apoptosis induced by HDAC6 inhibition, but it is not related to ER stress. We then looked at the nature of GRP78. GRP78 is the regulator of UPR, and traditionally exists in the ER lumen. Under ER stress, the expression of GRP78 is up-regulated [7, 19]. Interestingly, several reports have demonstrated that GRP78 is translocated from the ER to the cell plasma membrane under ER stress in various types of cancer, including breast cancer, colorectal cancer and prostate cancer [16, 20, 21].

Accordingly, we checked whether GRP78 was located on the plasma membrane in CCA and whether HDAC6 inhibition by ACY-1215 had any effect on the localization of GRP78. We first performed biotinylation assays. Biotins bind to the cell surface proteins, and then cell surface proteins labeled with the biotins can be purified by avidin agarose [22]. The TFK-1 cells were cultured with ACY-1215 10 μM for 24 hours. Through the biotinylation assay, we labeled and purified the GRP78 located on the plasma membrane and detected the GRP78 via western blot analysis. Compared with untreated cells, the density of GRP78 protein located on the plasma membrane was reduced by approximately 80% after treatment with ACY-1215 (Fig. 5A, B). We also stained for the GRP78 protein on

the cell surface with an anti-GRP78 antibody and analyzed it by FACS. Consistent with the biotinylation result, the level of GRP78 protein on the cell surface was reduced by approximately 30% under ACY-1215 (Fig. 5C, D).

We presumed that blockade of GRP78 translocation to the plasma membrane might be induced by the accumulation of acetylation on the GRP78 by inhibition of HDAC6 activity. To prove our hypothesis, we performed co-immunoprecipitations using anti-GRP78 and anti-acetyl-lysine antibodies. First, we checked whether the total amount of GRP78 was increased by ACY-1215 treatment (Fig. 5E left). Next, we checked the level of acetyl-lysine on GRP78 by immunoprecipitation. The level of acetyl-lysine was increased approximately 2-fold under ACY-1215 treatment (Fig. 5E middle, right). Taken together, ACY-1215 leads to the accumulation of acetylation on GRP78 through HDAC6 inhibition, which results in a decline of GRP78 expression on the cell membrane.

Figure 5

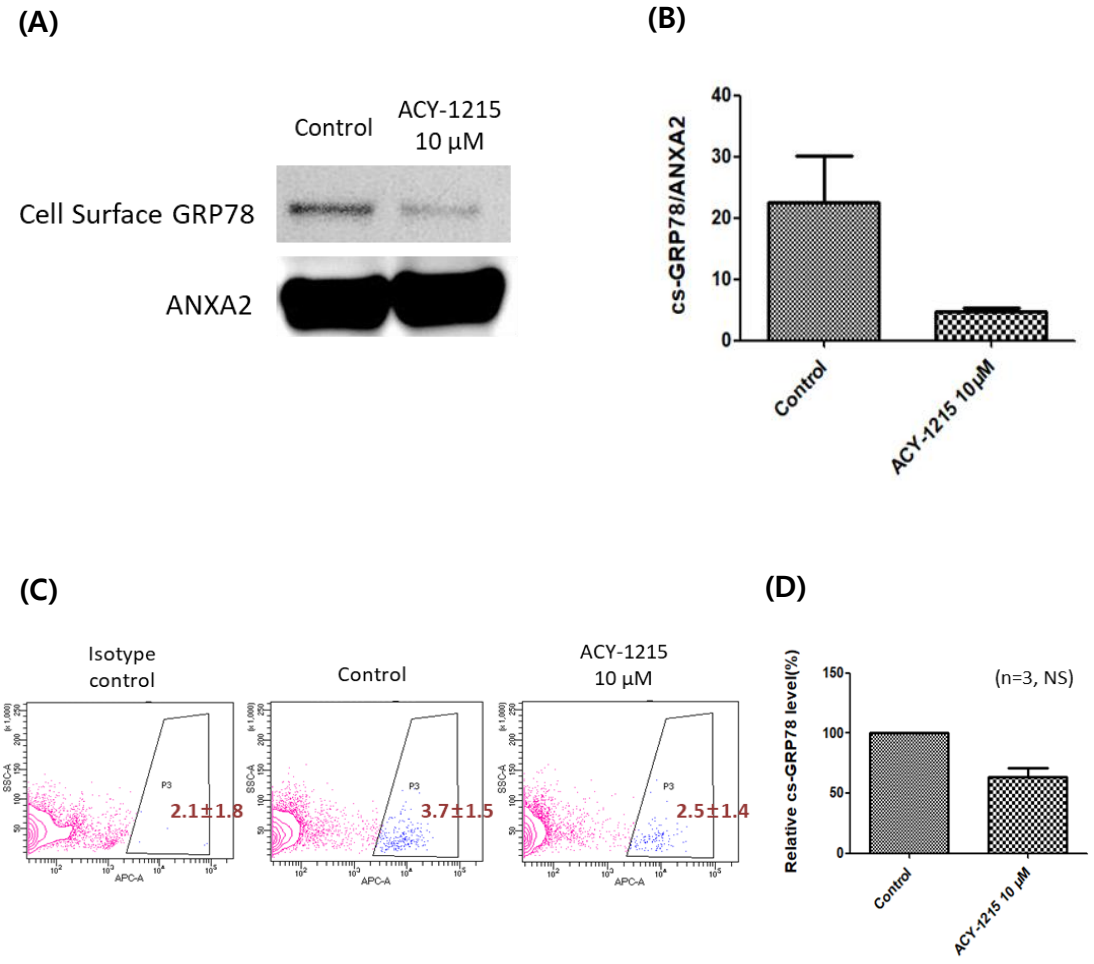
(A)
Control
ACY-1215 10 μM
Cell Surface GRP78
ANXA2
(B)
cs-GRP78/ANXA2
40
30
20
10
0
Control
ACY-1215 10μM
(C)
Isotype control
Control
ACY-1215 10 μM
P3
2.1±1.8
3.7±1.5
2.5±1.4
SSC-A
APC-A
(D)
Relative cs-GRP78 level(%)
150
100
50
0
(n=3, NS)
Control
ACY-1215 10 μM
(E)
20% input TCL
Control
ACY-1215 20 μM
GRP78
β-actin
IB
IP : GRP78
Control
ACY-1215 20 μM
Acetyl-lysine
GRP78
IP : Acetyl-lysine
Control
ACY-1215 20 μM
GRP78
Acetly-lysine

Figure 5. HDAC6 inhibition suppressed translocation of GRP78 to the cell surface via GRP78 acetylation. (A), (B) HDAC6 inhibition decreased distribution of GRP78 on the cell surface. Bars are expressed as the Ave ± STDEV from three independent experiments. (C) TFK-1 cells were either untreated (Control) or treated with 10 μM ACY-1215 for 24 hours. Cell surface GRP78 were measured by FACS. Pink dots, Isotype control; Blue dots, anti- GRP78 Ab. (D) Relative cell surface-GRP78 level of either untreated (Control) or treated with 10 μM ACY-1215 for 24 hours (n=3). (E) TFK-1 cells were either untreated (Control) or treated with 10 μM ACY-1215 for 24 hours. Subsequently, the lysates from the cell pellets were immunoprecipitated with anti-GRP78 antibody, anti-acetyl-lysine antibody respectively and immunoblotted for acetyl-lysine, GRP78 respectively. ACY-1215 treatment increased endogenous acetylated GRP78. Data shown here represent one of three independent experiments.

Absence of cell surface GRP78 induced by ACY-1215 promoted apoptosis via AKT/Bad signaling

A recent investigation has reported that GRP78 located on the cell surface promotes a wide array of cancer cell proliferation via PI3K/AKT signaling [14, 16] or drives apoptosis [6]. However, it is still unclear how the GRP78 located on the cell surface regulates cell proliferation or apoptosis in CCA. According to previous reports, phospho-AKT blocks apoptosis by phosphorylation of BAD, one of the pro-apoptotic BCL-2 family proteins, in nasopharyngeal carcinoma and oral cancer cells. In particular, the phosphorylation status of the serines at 112 and 136 on BAD are the critical points to change the fate of cells [23, 24].

First, we investigated AKT signaling under the condition of lacking cell surface GRP78 using ACY-1215. The cells were exposed to ACY-1215 at 5, 10 and 20 μM for 24 hours. Following this treatment, the phosphorylation level of Ser473 on AKT, a survival signal, was sharply decreased even at the lower concentrations of ACY-1215 (Fig. 6A). On the other hand, the phosphorylation level of The308 on AKT, blocking the signal of apoptosis via BAD phosphorylation, was also decreased in the cells exposed to ACY-1215 (Fig. 6B). Moreover, the phosphorylation of Bad on both Ser112 and Ser136 decreased in the cells exposed to ACY-1215 compared with untreated cells (Fig. 6B). These results

indicate that lacking cell surface GRP78 induced by HDAC6 inhibition by ACY-1215 regulates proliferation and apoptosis via AKT/Bad signaling in CCA.

Figure 6

(A)

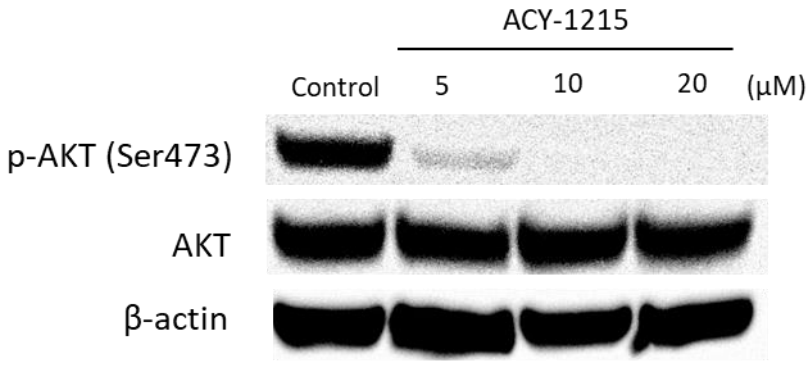
ACY-1215
Control
5
10
20
(μM)
p-AKT (Ser473)
AKT
β-actin

(B)

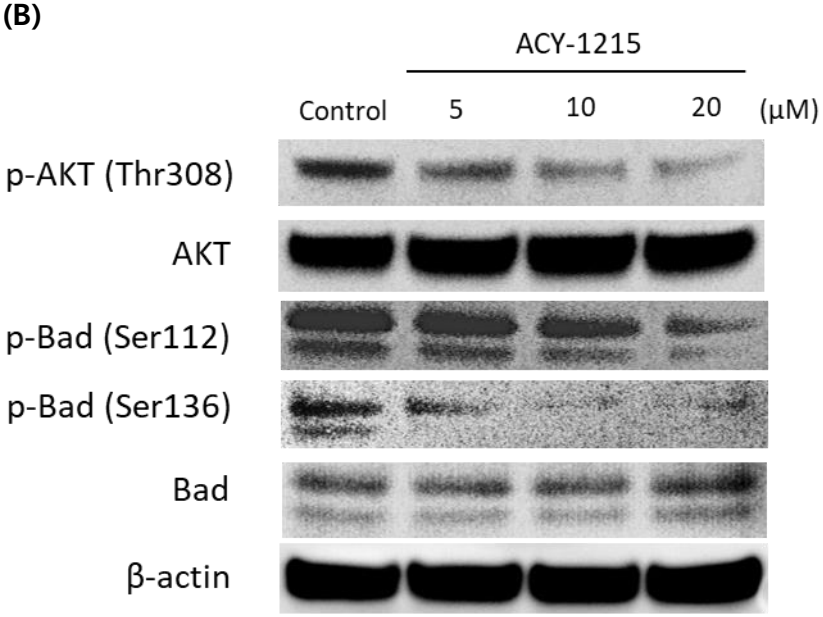
ACY-1215
Control
5
10
20
(μM)
p-AKT (Thr308)
AKT
p-Bad (Ser112)
p-Bad (Ser136)
Bad
β-actin

Figure 6. ACY-1215 suppressed proliferation and induced apoptosis via AKT/Bad signaling. (A) Following ACY-1215 treatment at the indicated concentrations (5, 10 and 20 μM) for 24 hours, p-AKT (Ser473) were detected by western blot. p-AKT (Ser473) related to proliferating signal of cancer cell. HDAC6 inhibition suppressed cell proliferation. Data shown here represent one of three independent experiments. (B) TFK-1 cells were treated with ACY-1215 at the indicated concentrations (5, 10 and 20 μM) for 24 hours. Western blot represented p-AKT (Thr308), AKT, p-Bad (Ser112), p-Bad (Ser136), Bad, B-actin. P-AKT (Thr308) related to blocking of apoptosis via Bad phosphorylation. HDAC6 inhibition also induced apoptosis.

HDAC6 inhibition suppressed tumor growth in a CCA xenograft model

Given the results so far, we uncovered the possibility of the GRP78 located on the plasma membrane to be a therapeutic target. Accordingly, we validated the therapeutic effects of ACY-1215 in a CCA xenograft model using TFK-1 cells. The group treated with ACY-1215 showed a statistically significant tumor growth inhibition by 46% compared to vehicle control at Day 76 (7 mice/group, $^{**}P < 0.01$) (Fig. 7A-D). The body weight changes of the animals indicated that toxicity was not observed in the ACY-1215 treatment or the control groups (Fig. 7E). We further analyzed the tumor cell proliferation (Ki-67) to evaluate the drug efficacy in the tumor tissues. Compared with the vehicle group, the expression of Ki-67 was higher in the group treated with ACY-1215 (Fig. 7F). Together, these findings indicate that ACY-1215 has therapeutic efficacy in vivo.

Figure 7

(A)

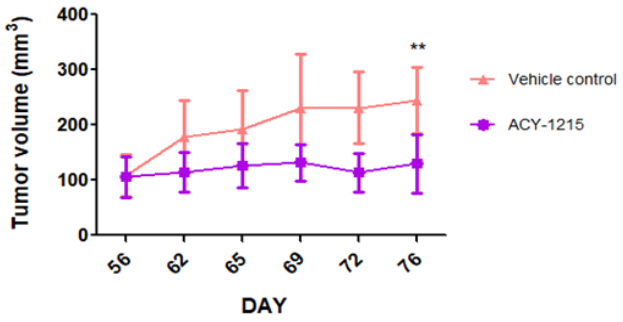

(B)

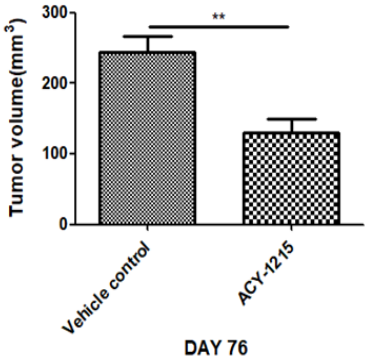

(C)

	Tumor volume (Ave±SD, mm^3)						
Day	0	56	62	65	69	72	76
	Cell implantation	grouping	7 day	10 day	14 day	17 day	21 day
Vehicel (5% DMSO)	0	108.3±37.8	179.1±65.2	191.7±71.5	230±97.9	231.3±65.9	244.7±59.6
ACY-1215 50mpk	0	106±37	114.6±35.8	127±40	131.5±33.3	114.2±34.8	130.1±53.1

(D)

(E)

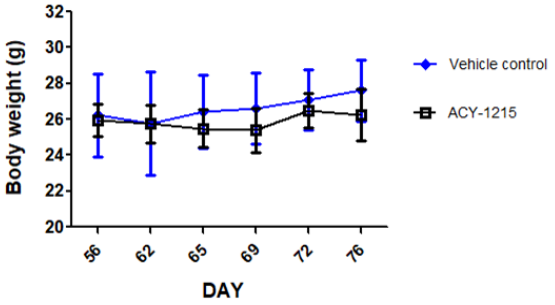

(F)

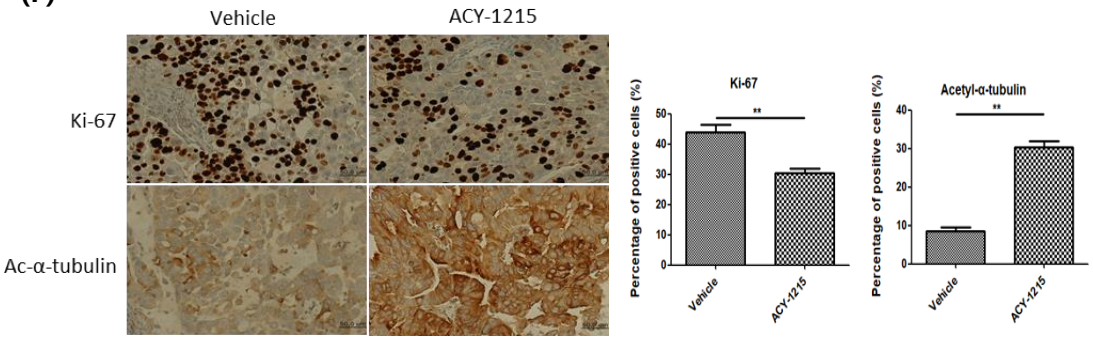

Figure 7. HDAC6 inhibition suppresses tumor growth in CCA xenograft model. (A) $5x10^6$ TFK-1 cells were implanted into the flank of Balb/c nude mouse. When average tumor volume reached $100mm^3$, Balb/c nude mice were treated with 5% DMSO + 45% PEG-400 + 50% ddH2O (Vehicle, n =7), ACY-1215 50 mg/kg (n=7), by i.p. injection for 3 weeks. Tumor growth was inhibited in the ACY-1215-treated group compared with controls (B) On day 76, tumor growth inhibition was 46% by ACY-1215 (n=7, $^{**}P < 0.01$ versus vehicle control group). (C) Table of average tumor volume. (D) Tumor volume was measured per 3~4 days/week for 3 weeks and there was a tumor growth inhibition in the relative tumor volume of ACY-1215 treated group when compared to the vehicle control group (n=7). (E) The body weight of mice after drug treatment up to day 76 (n=7). (F) Immunohistochemical expression of Ki-67 and Ac-α-tubulin. A representative of tumor tissues IHC stained with Ki-67, Ac-α-tubulin. Quantification analysis of IHC staining of Ki-67 and Ac-α-tubulin (scale bar = 100 μm, 40× magnification, $^{**}P < 0.001$, n = 3 for each).

Discussion

Our findings demonstrated that GRP78 acetylation by HDAC6 inhibition is a potential target for an anti-tumor effect in CCA. This study showed that: 1) CCA cells were more sensitive to ACY-1215, a HDAC6 selective inhibitor, than normal cholangiocytes. 2) Acetylation of GRP78 by ACY-1215 increased, which led to suppression of translocation of GRP78 to the cell surface. 3) ACY-1215 inhibited proliferation by decreasing p-AKT (Ser473) and induced apoptosis via AKT-Bad signaling. These data suggest crucial roles for HDAC6 and cell surface GRP78 in CCA.

Previous studies demonstrated the anti-tumor effect of pan-HDAC inhibitors, including vorinostat, TSA, VPA, and CG200745, in CCA [2-4]. We also found that the proliferation of TFK-1 cells was suppressed by SAHA (data not shown). However, we focused on the role of HDAC6 in CCA biology since it has been reported that HDAC6 and its substrates were closely associated with cancer [25-28].

To investigate their roles and the relationship between HDAC6 and GRP78, we treated CCA cell lines with ACY-1215. In general, it is well-known that HDAC6 inhibition induces ER stress through the failure to clear misfolded proteins [29, 30], with the result that ER stress-mediated apoptosis occurs after the induction of C/EBP homologous protein (CHOP) [31, 32]. Interestingly, our results showed ACY-1215 induced apoptosis (Fig. 3)

even though CHOP was not induced by ACY-1215 (data not shown). Furthermore, the level of ubiquitin, a general ER-stress pattern, also did not change, while ACY-1215 induced the activation of ER chaperones GRP78 and phospho-PERK (Fig. 4). With these observations, we thought that the phospho-PERK might act as a responder to alleviate ER-stress.

Among the ER chaperones, GRP78 is known to be a substrate of HDAC6. Actually, because cancer cells undergo prolonged ER-stress, we considered whether GRP78 has a crucial role in CCA survival. It has been reported that ER stress-induced GRP78 translocation to the plasma membrane contributes to the survival of cancer [8, 13, 14, 22]. The GRP78 translocation mechanism is that GRP78 contains a KDEL motif at the C-terminus, which retrieves GRP78 from the Golgi apparatus to the ER via the KDEL receptor. In effect, in a solid tumor under prolonged ER stress, the total amount of GRP78 exceeds the KDEL binding capacity of the KDEL receptor, and only some of the GRP78 is retrieved to the ER. The rest of the GRP78 translocates to the cell surface. Treatment with the anti-GRP78 antibody MAb159, which specifically recognizes surface GRP78, suppresses tumor growth in vitro and in vivo [14]. In addition, GRP78 modification by HDAC6 affects the location of GRP78 [33].

In effect, our data demonstrated the expression level of cs-GRP78 on the plasma membrane decreased (Fig. 5A-D) and the level of acetylation on GRP78 increased (Fig. 5E)

by treatment with ACY-1215. Liu R et al. have reported that cs-GRP78 regulated PI3K/AKT signaling upstream via the interaction of cs-GRP78 with p85, a subunit of PI3K [14]. AKT signaling regulates both proliferation and apoptosis according to the site of phosphorylation on AKT. Because cs-GRP78 acts as an α2-macroglobulin signaling receptor and interacts with PI3K, we looked for any alterations of the PI3K/AKT pathway, especially the phosphorylation sites of AKT, under ACY-1215 treatment. As expected, our findings showed alterations of AKT signaling. Both the proliferation signaling (Ser473 of AKT) and the anti-apoptotic signaling (Thr308 of AKT) were decreased (Fig. 6A). These alterations on AKT affected BAD, a pro-apoptotic protein. Phosphorylation of BAD by AKT, known as the main kinase regulating BAD, induces its sequestration from the mitochondria, resulting in a blockade of apoptosis [23, 24].

Furthermore, if CCA becomes resistant to HDAC6 inhibitors, our findings suggest that PI3K/AKT signaling can be targeted. It has been reported that there is a synergic effect between HDAC and PI3K inhibition in cancer cell death [34], but the involvement of cs-GRP78 remains unclear. The combination of an HDAC6 inhibitor with a PI3K/AKT inhibitor is one potential strategy to overcome HDAC6 inhibitor resistance.

Compared with the CCA cell lines, the MMNK-1 cells, normal cholangiocytes, had higher drug resistance to ACY-1216 (Fig. A). It has been discovered that HDAC6

contributes to shortened cilia or ciliary loss in CCA [5]. A longer cilia length is conferred by drug resistance to kinase inhibitors [35]. Based on previous studies, since the cilia of MMNK-1 cells are longer than that of CCA cells, ACY-1215 has less influence on normal bile ductal cell. Unfortunately, in our data, ciliary expression by the normal cholangiocytes and CCA cells was not confirmed. We plan to confirm the presence of cilia and determine whether the ciliary length or number is associated with sensitivity to ACY-1215.

In conclusion, our results suggest there is an association between HDAC6 and GRP78 on the plasma membrane, which promotes CCA growth and survival. We showed that blockade of GRP78 translocation to the plasma membrane via an increase in acetylated GRP78 by HDAC6 inhibition suppressed tumor growth and induced cell death of CCA in vitro and in vivo. Therefore, HDAC6 inhibitors could be a potential therapeutic approach to CCA.

Reference

1. Juan Valle , Harpreet Wasan, Daniel H Palmer, David Cunningham, Alan Anthoney, Anthony Maraveyas, et al. Cisplatin Plus Gemcitabine Versus Gemcitabine for Biliary Tract Cancer. N Engl J Med 2010;**362**:1273–81.

2. Takuya Sakamoto, Shogo Kobayashi, Daisaku Yamada, Hiroaki Nagano, Akira Tomokuni, Yoshito Tomimaru, et al. A Histone Deacetylase Inhibitor Suppresses Epithelial-Mesenchymal Transition and Attenuates Chemoresistance in Biliary Tract Cancer. PLoS One 2016;**11**:e0145985.

3. Joon Ho Wang, Eun Jeoung Lee, Meiying Ji, Seon Mee Park. HDAC Inhibitors, Trichostatin A and Valproic Acid, Increase E-cadherin and Vimentin Expression but Inhibit Migration and Invasion of Cholangiocarcinoma Cells. Oncol Rep 2018;**40**:346-54.

4. Dawoon E. Jung, Soo Been Park, Kahee Kim, Chanyang Kim, Si Young Song. CG200745, an HDAC Inhibitor, Induces Anti-Tumour Effects in Cholangiocarcinoma Cell Lines via miRNAs Targeting the Hippo Pathway. Sci Rep 2017;**7**:10921.

5. Sergio A Gradilone, Brynn N Radtke, Pamela S Bogert, Bing Q Huang, Gabriella B Gajdos, Nicholas F LaRusso. HDAC6 Inhibition Restores Ciliary Expression and Decreases Tumor Growth. Cancer Res 2013;**73**:2259–70.

6. Min Ni, Yi Zhang, Amy S Lee. Beyond the Endoplasmic Reticulum: Atypical GRP78 in Cell Viability, Signalling and Therapeutic Targeting. Biochem J 2011;**434**:181–8.

7. Hana Kim, Asmita Bhattacharya, Ling Qi. Endoplasmic Reticulum Quality Control in Cancer: Friend or Foe. Semin Cancer Biol 2015;**33**:25–33.

8. Yuan-Li Tsai, Yi Zhang, Chun-Chih Tseng, Ramunas Stanciauskas, Fabien Pinaud, Amy S Lee. Characterization and Mechanism of Stress-induced Translocation of 78-Kilodalton Glucose-regulated Protein (GRP78) to the Cell Surface. J Biol Chem 2015;**290**:8049–64.

9. Min Ni, Hui Zhou, Shiuan Wey, Peter Baumeister, Amy S Lee. Regulation of PERK Signaling and Leukemic Cell Survival by a Novel Cytosolic Isoform of the UPR Regulator GRP78/BiP. PLoS One 2009;**4**:e6868.

10. Shang-Pang Huang, Jung-Chou Chen, Chih-Chung Wu, Chi-Tsai Chen, Nou-Ying Tang, Yung-Tsuan Ho, et al. Capsaicin-induced Apoptosis in Human Hepatoma HepG2 Cells. Anticancer Res 2009;**29**:165–74.

11. Rong Fu, Peng Yang, Hai-Li Wu, Zong-Wei Li, Zhuo-Yu Li. GRP78 Secreted by Colon Cancer Cells Facilitates Cell Proliferation via PI3K/Akt Signaling. Asian Pac J Cancer Prev 2014;**15**:7245-9.

12. Rui Li, Gu Yanjiao, He Wubin, Wang Yue, Huang Jianhua, Zheng Huachuan, et al. Secreted GRP78 Activates EGFR-SRC-STAT3 Signaling and Confers the Resistance to Sorafeinib in HCC Cells. Oncotarget 2017;**8**:19354-64.

13. Zongwei Li, Zhuoyu Li. Glucose Regulated Protein 78: A Critical Link Between Tumor Microenvironment and Cancer Hallmarks. Biochim Biophys Acta 2012;**1826**:13–22.

14. Ren Liu, Xiuqing Li, Wenming Gao, Yue Zhou, Shiuan Wey, Satyajit Mitra, et al. Monoclonal Antibody Against Cell Surface GRP78 as a Novel Agent in Suppressing PI3K/AKT Signaling, Tumor Growth, and Metastasis. Clin Cancer Res 2013;**19**:6802–11.

15. Uma Kant Misra, Rohit Deedwania, Salvatore Vincent Pizzo. Binding of Activated alpha2-macroglobulin to Its Cell Surface Receptor GRP78 in 1-LN Prostate Cancer Cells Regulates PAK-2-dependent Activation of LIMK. J Biol Chem 2005;**280**:26278–86.

16. Xiaoli Yao, Hua Liu, Xinghua Zhang, Liang Zhang, Xiang Li, Changhua Wang, et al. Cell Surface GRP78 Accelerated Breast Cancer Cell Proliferation and Migration by Activating STAT3. PLoS One 2015;**10**:e0125634.

17. Hyun-Wook Ryu, Hye-Rim Won, Dong Hoon Lee, So Hee Kwon. HDAC6 Regulates Sensitivity to Cell Death in Response to Stress and Post-Stress Recovery. Cell Stress Chaperones 2017;**22**:253–61.

18. ACY-1215 Accelerates Vemurafenib Induced Cell Death of BRAF-mutant Melanoma Cells via Induction of ER Stress and Inhibition of ERK Activation. Oncol Rep 2017;**37**:1270-6.

19. Abhishek D Garg, Hannelore Maes, Alexander R van Vliet, Patrizia Agostinis. Targeting the Hallmarks of Cancer With Therapy-Induced Endoplasmic Reticulum (ER) Stress. Mol Cell Oncol 2014;**2**:e975089.

20. Zongwei Li, Lichao Zhang, Yarui Zhao, Hanqing Li, Hong Xiao, Rong Fu, et al. Cell-surface GRP78 facilitates colorectal cancer cell migration and invasion. Int J Biochem Cell Biol 2013;**45**:987–94.

21. Uma Kant Misra, Rohit Deedwania, Salvatore Vincent Pizzo. Activation and Cross-talk between Akt, NF-B, and Unfolded Protein Response Signaling in 1-LN Prostate Cancer Cells Consequent to Ligation of Cell Surface-associated GRP78. J Biol Chem 2006;**281**:13694–707.

22. Yi Zhang, Ren Liu, Min Ni, Parkash Gill, Amy S Lee. Cell Surface Relocalization of the Endoplasmic Reticulum Chaperone and Unfolded Protein Response Regulator GRP78/BiP. J Biol Chem 2010;**285**:15065–75.

23. S R Datta, H Dudek, X Tao, S Masters, H Fu, Y Gotoh, et al. Akt Phosphorylation of BAD Couples Survival Signals to the Cell-Intrinsic Death Machinery. Cell 1997;**91**:231–41.

24. Wai Kien Yip, Vincent Ching Shian Leong, Maizaton Atmadini Abdullah, Suryati Yusoff, Heng Fong Seow. Overexpression of phospho-Akt Correlates With Phosphorylation of EGF Receptor, FKHR and BAD in Nasopharyngeal Carcinoma. Oncol Rep 2008;**19**:319-28.

25. Shigehira Saji, Masayo Kawakami, Shin-Ichi Hayashi, Nobuyuki Yoshida, Makiko Hirose, Shin-Ichiro Horiguchi, et al. Significance of HDAC6 Regulation via Estrogen Signaling for Cell Motility and Prognosis in Estrogen Receptor-Positive Breast Cancer. Oncogene 2005;**24**:4531–9.

26. Shinji Tsutsumi, Kristin Beebe, Len Neckers. Impact of Heat-Shock Protein 90 on Cancer Metastasis. Future Oncol 2009;**5**:679–88.

27. Gang Ding, He-Dai Liu, Qian Huang, Hong-Xiang Liang, Zhao-Han Ding, Zhi-Jun Liao, et al. HDAC6 Promotes Hepatocellular Carcinoma Progression by Inhibiting P53 Transcriptional Activity. FEBS Lett 2013;**587**:880–6.

28. Kiminori Kanno, Shoji Kanno, Hiroyuki Nitta, Noriyuki Uesugi, Tamostu Sugai, Tomoyuki Masuda, et al. Overexpression of Histone Deacetylase 6 Contributes to Accelerated Migration and Invasion Activity of Hepatocellular Carcinoma Cells. Oncol Rep 2012;**28**:867-73.

29. Rekha Rao, Srilatha Nalluri, Ravindra Kolhe, Yonghua Yang, Warren Fiskus, Jianguang Chen, et al. Treatment with Panobinostat Induces Glucose-Regulated Protein 78 Acetylation and Endoplasmic Reticulum Stress in Breast Cancer Cells. Mol Cancer Ther 2010;**9**:942-52.

30. Yuying Feng, Rongshuang Huang, Fan Guo, Yan Liang, Jin Xiang, Song Lei, et al. Selective Histone Deacetylase 6 Inhibitor 23BB Alleviated Rhabdomyolysis-Induced Acute Kidney Injury by Regulating Endoplasmic Reticulum Stress and Apoptosis. Front Pharmacol 2018;**26**:274.

31. S Oyadomari, M Mori. Roles of CHOP/GADD153 in Endoplasmic Reticulum Stress. Cell Death Differ 2004;**11**:381–9.

32. Hai Hu, Mingxing Tian, Chan Ding, Shengqing Yu. The C/EBP Homologous Protein (CHOP) Transcription Factor Functions in Endoplasmic Reticulum Stress-Induced Apoptosis and Microbial Infection. Front Immunol 2019;**9**:3083.

33. Zongwei Li, Ming Zhuang, Lichao Zhang, Xingnan Zheng, Peng Yang, Zhuoyu Li. Acetylation Modification Regulates GRP78 Secretion in Colon Cancer Cells. Sci Rep 2016;**6**:30406.

34. Kaiming Sun, Ruzanna Atoyan, Mylissa A Borek, Steven Dellarocca, Maria Elena S Samson, Anna W Ma, et al. Dual HDAC and PI3K Inhibitor CUDC-907 Downregulates MYC and Suppresses Growth of MYC-dependent Cancers. Mol Cancer Ther 2017;**16**:285-99.

35. Andrew D Jenks, Simon Vyse, Jocelyn P Wong, Eleftherios Kostaras, Deborah Keller, Thomas Burgoyne, et al. Primary Cilia Mediate Diverse Kinase Inhibitor Resistance Mechanisms in Cancer. Cell Rep 2018;**23**:3042–55.

국문요약

히스톤 탈아세틸화효소 6 (Histone deacetylase 6, HDAC6)는 주로 세포질 (cytoplasm)에 존재하며, 여러 비-히스톤 (non-Histone) 기질 (α-tubulin, HSP90, GRP78 등)의 탈아세틸화를 통해 미접힘 단백질 증가와 같은 세포 내 스트레스 대응 기작에 관여한다. 특히 HDAC6 는 대장암, 비소세포성폐암 등 암세포에서 소포체 관련 분해 (ER-associated degradation, ERAD)과 같은 자기 보호 반응에서 중요한 역할을 하며 치료표적으로 떠오르고 있다. 담도암은 표준치료제가 없고, 세포독성 항암제에 대한 반응률이 낮은 악성 암 종이지만 발현빈도가 높지 않아 타 암 종에 비해 연구가 부족한 상황이다. 최근 HDAC6 가 담도암 환자의 조직에서 과발현되어 있고 과발현된 HDAC6 는 환자의 예후가 좋지 못하다는 선행 연구결과가 있었으나, 분자생물학적 기전에 대해서는 충분히 연구되어 있지 않다. 따라서, HDAC6 저해제, ACY-1215 를 이용하여 담도암의 생장과 사멸에서 HDAC6 의 기능을 규명하고 치료표적으로 HDAC6 의 유효성을 평가, HDAC6 저해제를 담도암 치료를 위한 항암 약물로서의 가능성을 제시하고자 한다.

TFK-1, SSP-25 와 같은 담도암 세포주는 정상 담도 세포주보다 HDAC6 저해제인 ACY-1215 에 대한 높은 감수성과 함께 ACY-1215 농도의존적 세포자멸사를 보여 주었다. 포도당 조절 단백질 78 (Glucose-

regulated protein 78, GRP78)은 주로 소포체 내에 존재하며, 소포체 스트레스 대응 기작에서 주요한 조절자 역할을 한다. 담도암을 포함한 여러 고형암에서는 영양결핍, 산소 제한, 높은 신진대사 요구로 지속적이고 꾸준한 ER-stress 상황에 적응하고 살아가고 있기 때문에 GRP78 의 발현량도 높고 세포막에 분포량도 많다. ACY-1215 에 의해 HDAC6 가 저해되었을 때 GRP78 의 세포막 분포도가 감소하는 것을 확인하였고, 이는 HDAC6 활성억제로 GRP78 의 탈아세틸화가 저해됨에 기인된 결과로, 이 결과는 아세틸화 된 GRP78 의 증가로 확인하였다. 세포막에 존재하는 GRP78 은 phosphatidylinositol-3-kinase (PI3K)/AKT 신호전달경로를 통해 AKT 를 인산화 시켜 암세포 생장과 생존을 조절한다는 보고가 있다. 실제로 ACY-1215 에 의해 GRP78 의 세포막 분포가 줄어든 경우, AKT 의 인산화가 줄어들었고 암 세포의 생장 신호가 꺼지며 담도암 세포주의 전체 생장률 감소를 보였다. 세포실험 결과를 바탕으로 TFK-1 세포주를 이용한 담도암 동물모델에 ACY-1215 를 이용, 약물표적으로서 HDAC6 의 유효성을 평가하였고 ACY-1215 투여에 의한 종양성장 억제효과를 확인하였다.

이 연구는 HDAC6 저해에 의해 GRP78 의 탈아세틸화가 저해되고, GRP78 의 아세틸화 증가는 소포체에 존재하는 GRP78 이 세포막으로의 이동을 막아 세포막의 GRP78 을 통해 조절되던 AKT 의 인산화가 감소되면,

결과적으로 담도암 세포주 생장을 억제하고 세포자멸사가 촉진됨을 시사한다.

이를 바탕으로 담도암 치료에 대한 표적으로 HDAC6 를 제안하고자 한다.